

Structural Investigation for Reinforcing Congestion Alleviation in Concrete Members and Connections

Structural Investigation for Reinforcing
Congestion Alleviation in Concrete Members
and Connections

By

Thomas Kang and Woosuk Kim

**CAMBRIDGE
SCHOLARS**

P U B L I S H I N G

Structural Investigation for Reinforcing Congestion Alleviation
in Concrete Members and Connections,
by Thomas Kang and Woosuk Kim

This book first published 2013

Cambridge Scholars Publishing

12 Back Chapman Street, Newcastle upon Tyne, NE6 2XX, UK

British Library Cataloguing in Publication Data
A catalogue record for this book is available from the British Library

Copyright © 2013 by Thomas Kang, Woosuk Kim

All rights for this book reserved. No part of this book may be reproduced, stored in a retrieval system, or transmitted, in any form or by any means, electronic, mechanical, photocopying, recording or otherwise, without the prior permission of the copyright owner.

ISBN (10): 1-4438-5236-8, ISBN (13): 978-1-4438-5236-4

TABLE OF CONTENTS

List of Figures.....	vii
List of Tables.....	ix
Abstract	xi
Chapter One.....	1
Introduction	
1.1 Background	
1.2 Goal and Need for This Study	
Chapter Two	5
Literature Review	
2.1 Steel Fibers in Reinforced Lightweight Concrete Beams	
2.2 Reinforced Concrete Beam-Column Connections with Headed Bars	
Chapter Three.....	21
Hypotheses and Objectives	
Chapter Four.....	25
Structural Investigation of Steel Fiber-Reinforced Lightweight Concrete Beams	
4.1 Introduction	
4.2 Experimental Program	
4.3 Observations and Test Results	
4.4 Design Shear Strength of SFRLC Beams without Stirrups	
4.5 Summary	
Chapter Five	65
Structural Investigation of Prestressed Self-Consolidating Concrete Beams and Girder	
5.1 Introduction	
5.2 Experimental Program and Results	
5.3 Comparison with Numerical Analysis Results	
5.4 Summary	

Chapter Six	93
Structural Investigation of Reinforced Concrete Connections with Headed Bars under Seismic Loads	
6.1 Introduction	
6.2 Experimental Program	
6.3 Analysis of Test Results	
6.4 Summary	
Chapter Seven.....	125
Conclusion	
References	129

LIST OF FIGURES

- 1-1 L-joint of bent cap of I-35 overpass in Oklahoma City, OK and T-joint of I-35 substructure
- 1-2 Collapse due to outrigger knee joint failure during 1989 Loma Prieta Earthquake (Wikipedia, fn. USGS)
- 2-1 Modulus of rupture testing (per ASTM C1609) of concrete prisms (using Forney machine in Fears Lab at the University of Oklahoma [OU])
- 2-2 Compressive strength tests of SFRLC cylinders per ASTM C496, with two strain gauges attached to measure strains (using Forney machine in Fears Lab at the OU)
- 2-3 Schematic of shear specimen (Adapted from Balaguru and Dipsia, 1993)
- 2-4 Elevation and section of test beam (Adapted from Swamy et al., 1993)
- 2-5 Details of test slab specimen (Adapted from Theodorakopoulos & Swamy, 1993)
- 2-6 Flexural toughness test setup (Adapted from Higashiyama and Banthia, 2008)
- 2-7 Direct shear test setup (Adopted: Higashiyama and Banthia, 2008)
- 2-8 Headed deformed reinforcing bar requirement for bearing of deformation (Reproduced; ACI 318-08, 2008)
- 2-9 Failure modes for headed anchors (Reproduced; ACI 318-08, 2008)
- 2-10 Shallow embedment pullout test setup
- 2-11 Comparison of embedment depth h_d and bonded length l_b in concrete (Adapted from DeVries et al., 1999)
- 2-12 Edge distance and head parameters (Adapted from DeVries et al., 1999)
- 2-13 Pullout cone failure
- 2-14 Schematic of test specimen and setup (Reproduced; Wright and McCabe, 1997)
- 2-15 Location of headed and hooked bars (Reproduced from ACI 352-02, 2002)
- 2-16 Schematic diagrams of investigated beam-column connections
- 3-1 Potential solutions to alleviating steel congestion in concrete structures
- 3-2 Headed bars, steel fibers, and self-consolidating concrete
- 4-1 Test setup and test beams
- 4-2 Concrete compressive stress-strain curve for all specimens
- 4-3 MOR test
- 4-4 Tensile strength testing of longitudinal deformed bar
- 4-5 Details for hooked steel fibers used in this study and various steel fibers shapes
- 4-6 Schematics of sequential crack patterns (Numbers along the beam: distance from the mid-span [mm]; Numbers on the beam: load tons)]
- 4-7 Load-deflection relationships for SFRLC and SFRC
- 4-8 Comparison of shear load-deflection relationships between SFRC and SFRLC with $V_f = 0.5\%$
- 4-9 Load-bar strain relationship for SFRLC and SFRC

- 4-10 Comparison of shear load-bar strain relationships
- 4-11 Measured shear stresses versus shear span-to-depth ratio (a/d)
- 4-12 Measured moment at peak versus steel fiber volume fraction (V_f)
- 4-13 Design consideration of lightweight concrete modification factor λ based on research by Hanson (1961)
- 4-14 Measured shear strength (v_u) / calculated shear strength (v_n) versus main parameters
- 5-1 Details of prestressed SCC member sections
- 5-2 Elevations of the prestressed members
- 5-3 Slump flow test
- 5-4 Concrete compressive stress-strain curve for $R1$ and $I1$
- 5-5 Concrete compressive stress-strain curve for $R2$ and $I2$
- 5-6 Tensile normal stress at mid-span bottom versus prism displacement relationship for $R1$ and $I1$
- 5-7 Tensile normal stress at mid-span bottom versus prism displacement relationship for $R2$ and $I2$
- 5-8 Stress-strain relationships for longitudinal deformed bars
- 5-9 Stress-strain relationships for prestressing steel strands
- 5-10 Prestressing of 13 mm ($\frac{1}{2}$ in.) diameter low relaxation strands with a hydraulic jack at Coreslab Structures, Inc., Oklahoma City, Oklahoma
- 5-11 Test setup at the Donald G. Fears Engineering Laboratory in OU
- 5-12 Beam failures and cracking patterns at mid-span
- 5-13 Load-deflection at mid-span relationship
- 5-14 Load-deflection at mid-span relationship between experimental and numerical results
- 6-1 Dimensions and details for JH-R1 and JH-R2
- 6-2 Heads and threaded connections
- 6-3 Progress of fabricating specimens
- 6-4 Stress vs. strain curve for concrete compressive strength tests
- 6-5 Tensile normal stress at mid-span bottom versus prism displacement relationship for MOR tests
- 6-6 Stress-strain relationship for D19 (No. 6) longitudinal deformed bars
- 6-7 Test setup and dimensions for instrumentation
- 6-8 Overview of JH-R2 test specimen and setup
- 6-9 Loading history
- 6-10 Moment vs. drift ratio relationships for JH-R1
- 6-11 Moment vs. drift ratio relationships for JH-R2
- 6-12 Backbone envelopes of lateral load-drift relations
- 6-13 Beam moment vs. beam rotation relationships for JH-R1 and JH-R2 specimens
- 6-14 Normalized joint shear vs. joint shear distortion relationships for JH-R1 and JH-R2 specimens
- 6-15 Crack patterns at the end of seismic testing

LIST OF TABLES

- 4-1 Descriptions of test specimens
- 4-2 Relations between steel fiber dosage rate and volume fraction (V_f)
- 4-3 Physical characteristics of Type I Portland cement
- 4-4 Physical properties of coarse and fine aggregates
- 4-5 Chemical compositions of expanded clay aggregate
- 4-6 Physical properties of high-range water reducing admixture
- 4-7 Physical characteristics of SFRLC and SFRC mixtures
- 4-8 Measured material properties of SFRLC and SFRC
- 4-9 Physical properties of flexural reinforcing bars
- 4-10 Physical properties of steel fiber
- 4-11 Test results and failure modes of specimens
- 4-12 Design constant needed for lightweight concrete modification factor (λ), proposed based on the research by Hanson (1961)
- 4-13 Comparisons of measured peak shear strengths and shear strength capacities calculated based on the available SFRC shear strength models except for the replacement of f'_c by $\lambda^2 f'_c$ for SFRLC beams
- 4-14 Steepness (slope) of the linear regression line for the ratio of measured peak shear strength (v_u) to calculated shear strength (v_n), with the consideration of lightweight concrete factor ($\lambda = 0.75$)
- 5-1 SCC mixture proportions
- 5-2 Fresh and hardened concrete properties for SCC mixtures
- 5-3 Experimental results of prestressed SCC members
- 5-4 Material parameters used 2D modeling
- 5-5 Summary of experimental and numerical simulation results
- 6-1 Dimensions for heads and headed bars
- 6-2 Connection design parameters
- 6-3 Provided and required development lengths for headed beam bars used for connection subassemblies
- 6-4 Fresh and hardened concrete properties
- 6-5 Measured steel material properties
- 6-6 Instrumentation lists
- 6-7 Summary of seismic test results of moment and drift
- 6-8 Comparisons between test results and ACI 374.1-05 acceptance criteria
- 6-9 Comparison of maximum joint shear demands and nominal joint shear strengths

ABSTRACT

Since the beginning of this research, the authors have endeavored to determine how to resolve the issues involving steel congestion in reinforced concrete (RC) structures. Three potential solutions to this problem were researched in detail. In the first method, reinforced concrete (RC) was mixed with steel fibers. The use of steel fibers instead of shear reinforcement stirrups resulted in the reduction of reinforcing congestion in a manner which was both effective in reducing the effects of congestion and which was practical to implement. In the second method, steel congestion in reinforced concrete (RC) was effectively reduced by the use of self-consolidating concrete (SCC), which does not require the use of vibrators in its casting. In the final method, reinforcing congestion was effectively reduced by the use of headed bars instead of traditional hooked bars. These first and third approaches are emerging as a research topic of special interest in the American Concrete Institute (ACI).

In evaluating these three approaches, and in combining them in this study, varied types of concrete were used. Shear testing was conducted using a lightweight concrete mix. Flexural testing of lightweight prestressed concrete (PC) beams was conducted using self-consolidating concrete (SCC). Seismic testing of headed bars in RC beam-column connections was conducted using a normalweight concrete mix. These three experiments were the subject matter of this study. In these studies the experimental results were compared with the ACI 318-08 provisions and with existing modeling equations proposed by many researchers. New models were proposed which better correlated with the test results.

Therefore, although other studies in the world may have dealt with the alleviation of reinforcing congestion in RC and/or PC structures, in researching these three unique methods for the alleviation of reinforcing congestion it was discovered that several variations and combinations of such methods can provide effective solutions for diverse conditions. Most of all, this study should prove important in providing the basis for additional research since the guidelines and codes regarding the alleviation of reinforcing congestion are shown to be based upon previously limited data.

CHAPTER ONE

INTRODUCTION

1.1 Background

Over the last half-century, the reinforced and prestressed concrete structure industry has struggled with problems associated with reinforcement congestion and a lack of bar anchorage space. Continuous design code changes to accommodate resistance to heavy traffic (e.g., moving truck loads) or extreme hazards (such as earthquake actions) led to the increased use of large diameter reinforcing bars (e.g., D32, D36 or D43 [No. 10, 11 or 14]) for reinforced and prestressed concrete structures. As the size of the reinforcement increased, its development length also increased, intensifying the congestion problem.

It is well known that required development length is a function of the bar diameter. As such, the use of 90-degree standard hooks has been inevitable to ensure sufficient development length at the region where large diameter reinforcing bars terminate (Figure 1-1). It is recognized that straight bar termination with insufficient embedment from the critical section is extremely dangerous. Anchorage failure does not only preclude the development of the design moments and shear forces of the members, but also may result in catastrophic collapse due to the lack of structural integrity (Figure 1-2).

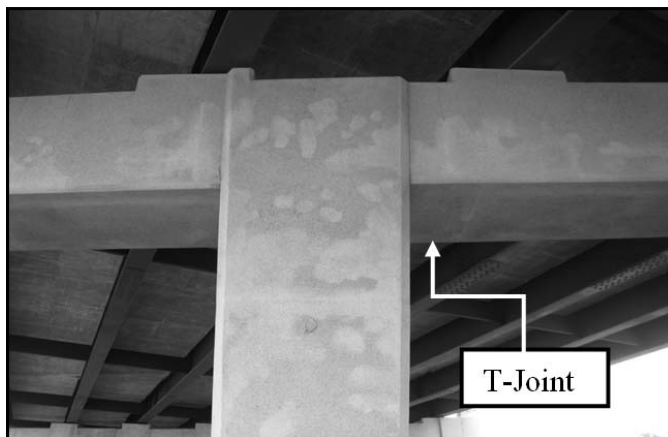
This also can happen in the case of hooked bar anchorage as a result of misdetermination of the required development length of reinforcement. It is generally required either that the depth of the bent cap be greater than that needed to fully develop the yield stress of straight column longitudinal reinforcement, or that hooked bars with sufficient development length be used. Similar requirements should apply to bent beam bars (Thompson et al., 2005) or at bridge pier-footing joints (Lehman et al., 2001). This important issue has been overlooked so that the bent cap joint or pier-foundation joint lacked room for large-diameter hooked bars.

Past earthquakes have allowed researchers to identify the aforementioned problems. The collapse of an 18-span viaduct during the 1995 Kobe earthquake in Japan (Yashinsky and Karshenas, 2003) was due

to insufficient development length of the longitudinal welded bars. A number of knee joint shear failures, accelerated by improper bar development, occurred during the 1989 Loma Prieta earthquakes (Figure 1-2). Such designs have clearly proven inadequate, and must be prevented from recurring in future design and construction.



(a) L-joint of bent cap of I-35 overpass in Oklahoma City, OK



(b) T-joint of I-35 substructure

Figure 1-1: L-joint of bent cap of I-35 overpass in Oklahoma City, OK and T-joint of I-35 substructure



Figure 1-2: Collapse due to outrigger knee joint failure during 1989 Loma Prieta Earthquake (Wikipedia, fn. USGS)

It is also essential to ensure the quality of cast-in-place concrete in steel-congested beam ends and beam-column connections such that the beams and connections of concrete structures are able to withstand natural and man-made hazards (e.g., earthquakes or blasts). As such, alleviation of reinforcing steel congestion without sacrificing structural performance is targeted this study.

1.2 Goal and Need for This Study

The primary goals of this study are to experimentally investigate both existing and new means to achieve steel congestion alleviation without sacrificing structural performance and to analytically develop pertinent design guidelines through data analysis. Three methods toward relieving the potential steel congestion in reinforced and prestressed concrete structures are proposed: use of headed bars, use of steel fibers in conjunction with lightweight aggregates, and use of self-consolidating concrete (SCC). These materials are becoming preferred choices in recent cast-in-place and precast construction. A new code development effort regarding the performance of the concrete in conjunction with these materials has been initiated and is still in its infant stage. The current research will contribute to the code development.

This book consists of seven chapters as follows:

- Chapter 1 is the introduction.
- Chapter 2 provides a review of previous literatures in the area.
- Chapter 3 presents the hypotheses and objectives of each study used.
- Chapter 4 shows the shear testing and analysis of steel fiber-reinforced lightweight concrete beams.
- Chapter 5 presents the experimental and analytical studies of prestressed self-consolidating concrete beams.
- Chapter 6 shows the seismic testing of exterior beam-column connections with closely-spaced headed bars.
- Chapter 7 provides the summary and conclusions of this study

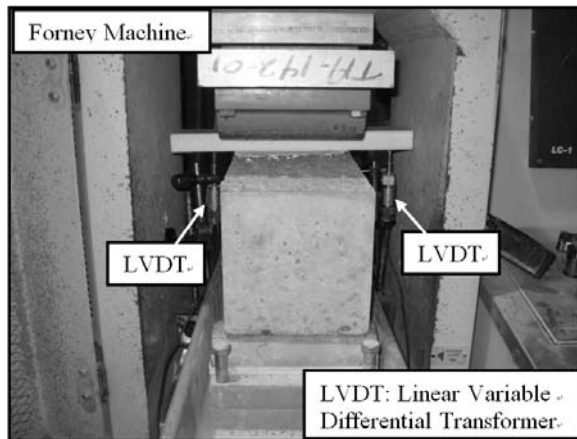
CHAPTER TWO

LITERATURE REVIEW

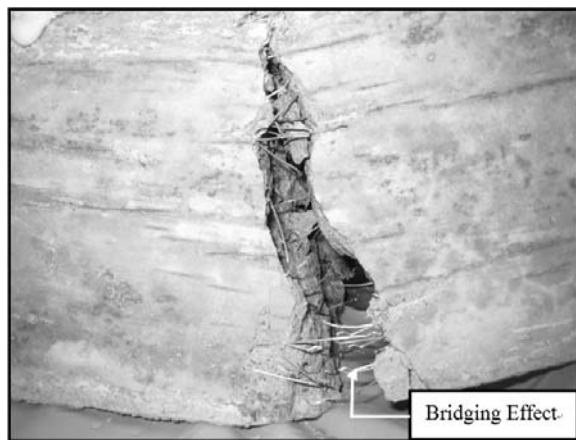
This chapter reviews the previous literature. Among several potential solutions to steel congestion in reinforced and prestressed concrete structures, this study examines three ways to achieve steel congestion alleviation: use of steel fiber-reinforced lightweight concrete (SFRLC), use of self-consolidating concrete (SCC), and use of headed bars. As there is little available research as to SCC, the literature review of SCC is excluded from this chapter. This literature review chapter focuses on the use of steel fibers in lightweight concrete beams and headed bars in reinforced concrete beam-column connections.

2.1 Steel Fibers in Reinforced Lightweight Concrete Beams

To date, studies on the use of steel fibers in lightweight concrete have been sparse. Most previous tests of SFRLC materials were performed using $100 \times 100 \times 360$ mm ($4 \times 4 \times 14$ in., appx.) prisms, 150×300 mm (6×12 in.) cylinders, and/or small-scale shear specimens (e.g., $80 \times 80 \times 155$ mm; $3 \times 3 \times 6$ in.) (Balaguru et al., 1987, 1993, 1996; Swamy and Jojagha, 1982a, 1982b; Kayali et al., 1999) (refer to Figures 2-1 to 2-3). Only two large-scale structural testing programs of SFRLC members were previously undertaken, one by Swamy et al. (1993) and the other by Theodorakopoulos and Swamy (1993). The following subsections provide a summary of prior experimental research on both large-scale structural testing and small-scale material testing of SFRLC.

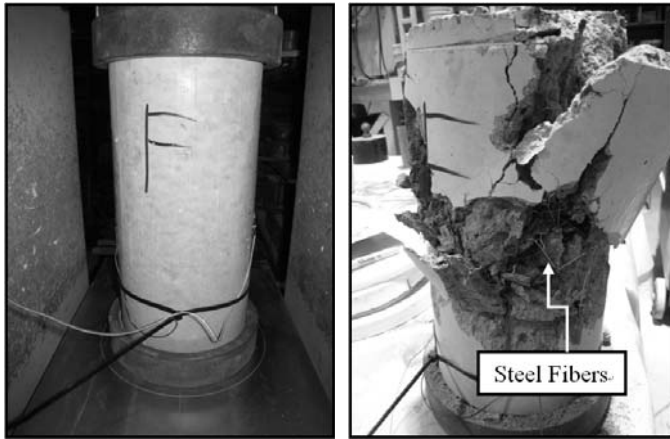


(a) Before test



(b) After test

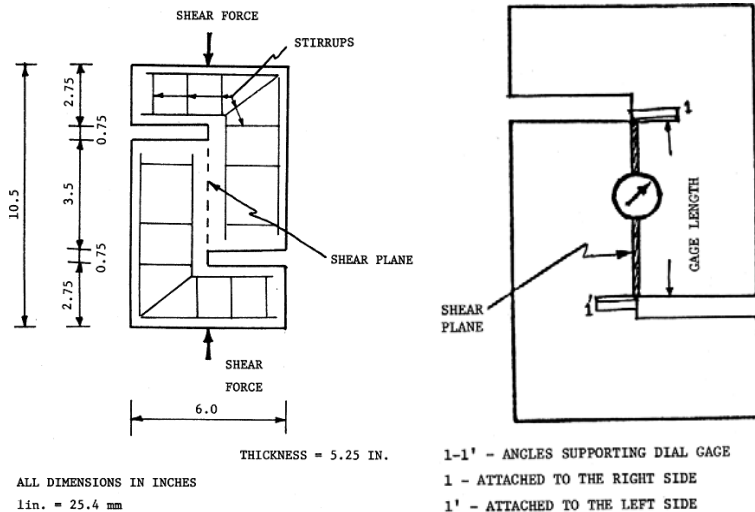
Figure 2-1: Modulus of rupture test (per ASTM C1609) of concrete prisms (using Forney machine in Fears Lab at the University of Oklahoma [OU])



(a) Before test

(b) After test

Figure 2-2: Compressive strength tests of SFRLC cylinders per ASTM C496, with two strain gauges attached to measure strains (using Forney machine in Fears Lab at the OU)



(a) Dimensions of double-L shear specimens (b) Shear specimens: location of dial gauge

Figure 2-3: Schematic of shear specimens (Adapted from Balaguru and Dipsia, 1993)

2.1.1 Part I: Experimental Research for Large-Scale Structural Testing

Swamy et al. (1993) tested eighteen large-scale specimens of SFRLC I-section beams with a span length of 3 m (118 in.) (Figure 2-4). The main variables studied were the shear span-to-depth ratio ($a/d = 2, 3.4, \text{ and } 4.9$), steel fiber volume fraction ($V_f = 0 \text{ and } 1\%$), and reinforcing ratio of bottom bars ($\rho = 1.6, 2.8, \text{ and } 4.3\%$). The test results indicated that the ultimate shear strength was dependent upon a/d and ρ , and that SFRLC with $V_f = 1\%$ showed significantly greater shear strength (by 60 to 210%) than equivalent beams without steel fibers. A shear strength design equation was developed based on the truss model and test data of their nine and others' previous 24 SFRC specimens (Swamy et al., 1993). This equation, which will be used for analysis in this prospectus, was also shown to correspond well to their seven SFRLC specimens (mean ratio of tested to predicted strength = 0.95; standard deviation = 0.11).

Theodorakopoulos and Swamy (1993) investigated the punching shear behavior and strength of SFRLC slab-column connections (Figure 2-5). Twenty connection specimens were tested for variables of steel fiber types (crimped, rectangular sectional, hooked, and paddle types), V_f (0.5 and 1%), reinforcing ratios of tension and compression slab steel (0.32 and 0.57%), column size (100, 150 and 200 mm; 4, 6 and 8 in.), and concrete compressive strength ($f'_c = 17.8 \text{ to } 58.6 \text{ MPa; } 2.6 \text{ to } 8.5 \text{ ksi}$). Overall, the addition of steel fibers in SFRLC slab-column connections increased the gravity load at first cracking (by 33 to 50%), at yielding (by 12 to 80%), and at punching (by 30 to 100%). Usage of paddle steel fibers with $V_f = 1\%$ resulted in the greatest punching shear strength.

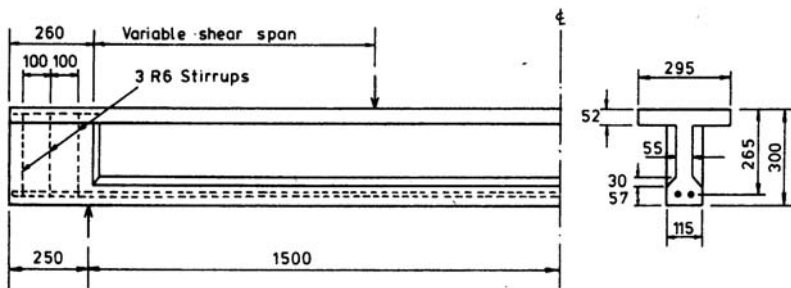


Figure 2-4: Elevation and section of test beam (Adapted from Swamy et al., 1993: Conversion: 1 mm = 0.039 in.)

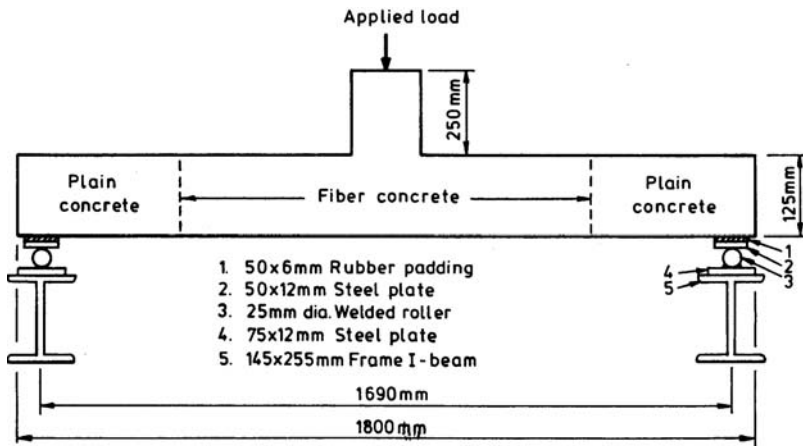


Figure 2-5: Details of test slab specimen (Adapted from Theodorakopoulos and Swamy, 1993; Conversion: 1 mm = 0.039 in.)

2.1.2 Part II: Experimental Research for Small-Scale Material Testing

Experimental studies were conducted by Balaguru et al. (1993, 1996) to assess the applicability of discrete steel fibers for improving the mechanical properties of normal-strength (42 MPa; 6 ksi) and high-strength (62.1 MPa; 9 ksi) lightweight concrete. The experimental programs consisted of three-point loading tests of prisms per ASTM (American Standard for Testing and Materials) C1018 (1993), splitting tensile and compressive strength tests of cylinders per ASTM C496/496M (2008), and direct shear tests. In their experimental studies, it was found that the addition of steel fibers to lightweight concrete increased the compressive strength (f'_c) by 7 to 70%, splitting tensile strength (f_{ct}) by 10 to 170%, and modulus of elasticity (E_c) by up to 65%. Also, SFRLC exhibited excellent flexural ductility and shear strength. These improved mechanical properties were observed for all combinations of the fiber aspect ratios (60, 75, and 100) and steel fiber volume fractions (0.55, 0.75, 0.9 and 1.1%).

Higashiyama and Banthia (2008) evaluated relationships between shear and flexural toughness for both SFRC and SFRLC. Materials used for their research consisted of two types of lightweight coarse aggregates (pumice and expansive shale), and two different lengths (38 and 63.5 mm; 1.5 and 9.2 in.) of crimped steel fibers with 1 mm (0.039 in.) diameter.

Two fiber volume fractions ($V_f = 0.5$ and 1%) were selected for four-point loading tests in accordance with ASTM C1609 (2008) (Figure 2-6) and for direct shear tests (Figure 2-7). The test results indicated that there was a linear relationship between shear and flexural strength for both SFRC and SFRLC, and that for a given fiber type and volume fraction, SFRC exhibited better shear and flexural toughness properties than SFRLC.

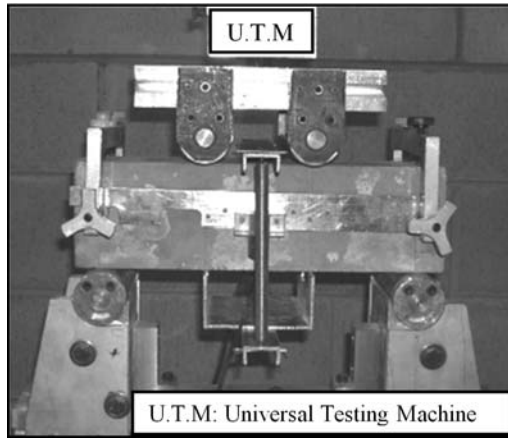
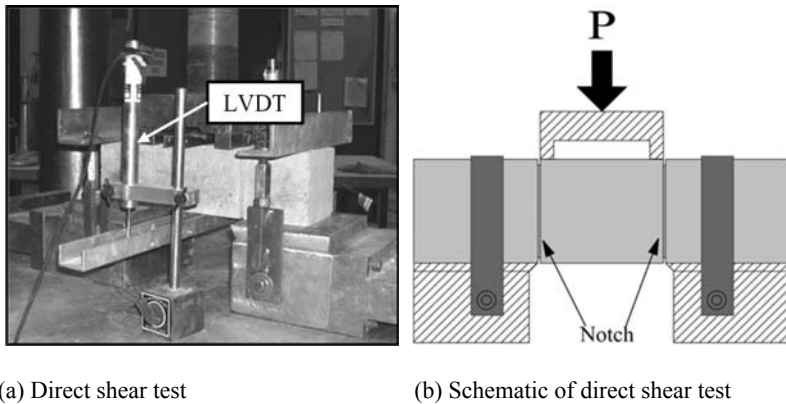


Figure 2-6: Flexural toughness test setup (Adapted from Higashiyama and Banthia, 2008)



(a) Direct shear test

(b) Schematic of direct shear test

Figure 2-7: Direct shear test setup (Adapted from Higashiyama and Banthia, 2008)

Swamy and Jojagha (1982a) performed a variety of workability tests for both SFRC and SFRLC in the fresh state, including inverted slump cone tests, standard slump and flow table tests, and vibrator-based remolding (VB) tests. Four different types of steel fibers (plain, paddle, hooked, and crimped) and four (length-to-diameter) aspect ratios of steel fiber ranging between 50 and 100 were tested. Both SFRC and SFRLC with $V_f = 1.0\%$ showed relatively poor workability, and it was concluded that pulverized fuel ash (PFA) and water-reducing-plasticizing admixture should be added to release inter-locking friction between fibers and aggregates. From the similar tests of Balaguru and Ramakrishnan (1987), it was concluded that toughness and energy absorption for SFRLC were equivalent to those for SFRC.

Swamy and Jojagha (1982b) experimentally assessed material characteristics of SFRC and SFRLC under impact loads by means of drop hammer and drop ball tests in accordance with ACI 544R-78 (1978). Three and four mixes were tested for normal weight and lightweight concrete, respectively. Both SFRC and SFRLC with $V_f = 1\%$ had greater impact resistance than those without steel fibers by a substantial degree, up to a factor of 10. The effects of steel fiber shape and geometry were evident by the fact that the number of shocks needed to fail was 536 and 793 for paddle and hooked shapes, respectively, but much less (124 and 192) for crimped and plain shapes.

2.2 Reinforced Concrete Beam-Column Connections with Headed Bars

This section briefly describes the existing literature of experimental tests of reinforced concrete beam-column connections with headed bars, and a review of ACI standards and recommendations (2008). The literature review of the anchorage details is also included to emphasize the behavior of heads used to transmit structural loads by bearing. This section consists of two parts: Part I summarizes ACI standards and recommendations, and Part II summarizes experimental research programs.

2.2.1 Part I: ACI Standards and Recommendations

In 2008, new provisions for headed bars were added to ACI 318. Sections 12.6.1 and 12.6.2 detail the development of headed bars and the limiting conditions for use of headed bars. ACI 318-08 (2008) also introduces new provisions (Section 3.5.9) for obstructions or interruptions of the bar deformations, which should not extend more than $2d_b$ from the

bearing face of the head (Figure 2-8). ASTM A970/A970M-07 (2007) “Standard Specification for Headed Steel Bars for Concrete Reinforcement,” should also be satisfied by the requirements of Section 3.5.9.

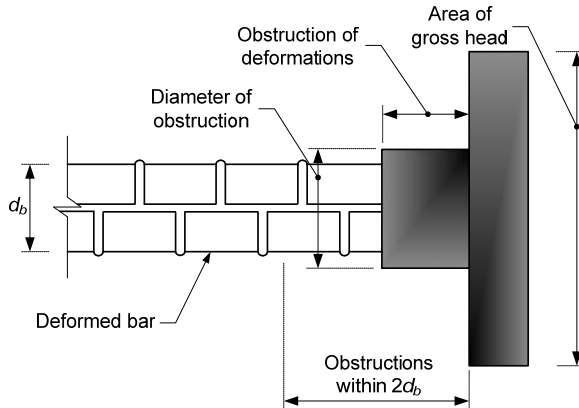


Figure 2-8: Headed deformed reinforcing bar requirements for bearing of deformation (Reproduced; ACI 318-08, 2008)

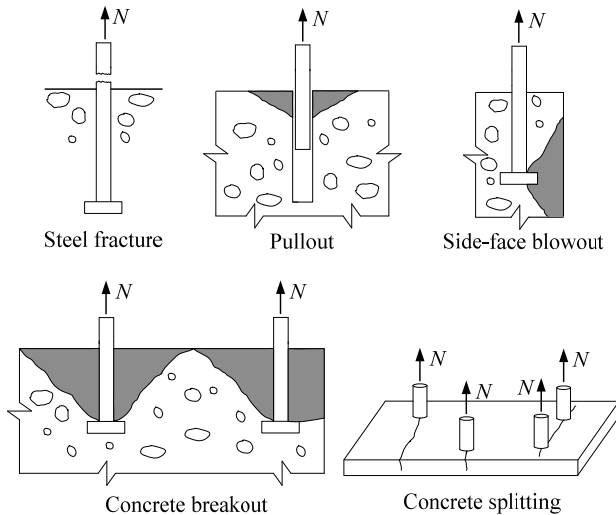


Figure 2-9: Failure modes for headed anchors (Reproduced; ACI 318-08, 2008)

ACI 318-08 (2008) Appendix D provides guidelines for the design of plain headed bars and headed anchors, bolts, or headed anchors in concrete. In ACI 318-08 (2008) Appendix D, the concrete capacity design (CCD) methodology is used to determine the anchorage capacity of headed anchors installed in mass plain concrete. In the CCD method, no bond stress is assumed along the length of a bar, and the concrete is assumed to be unconfined. ACI 318-08, Appendix D also describes the typical failure modes for steel elements with anchors under tensile and shear loading. Figure 2-9 shows the typical failure modes of steel anchors in tension.

Design guidelines for headed bars in beam-column connections were incorporated into the 2002 edition of the ACI 352R report on the basis of both monotonic (DeVries et al., 1999; Bashandy, 1996; Wright and McCabe, 1997) (or repeated (Bashandy, 1996)) and reversed cyclic tests (Wallace et al., 1998; Bashandy, 1996). To summarize briefly some of their experiments, DeVries et al. (1999) reported experimental test results on the anchorage capacity behavior based on several factors. These factors include the embedment depth, clear cover to the bar, orientation of the bar, the head geometry and dimension, and the anchorage region details (see Figures 2-10 to 2-12). A total of 150 headed bar pullout tests were performed with varying embedment-to-depth ratio, edge distance, head size and bar diameter, transverse reinforcement details, development length, and concrete compressive strength. Figure 2-13 shows one of the typical pullout failures of a shallow embedded headed reinforcing bar.

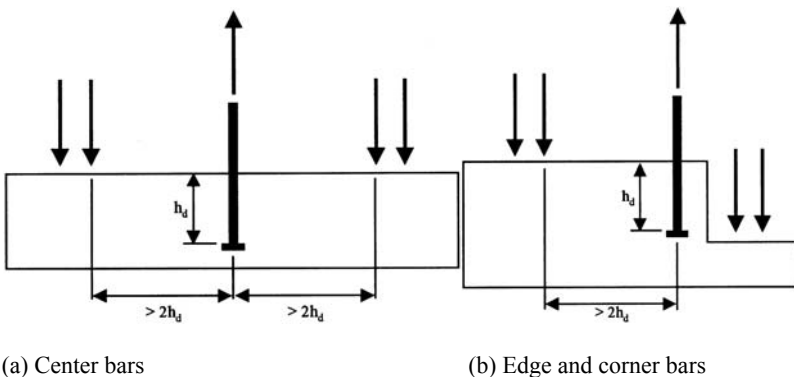


Figure 2-10: Shallow embedment pullout test setup (Adapted from DeVries et al., 1999)

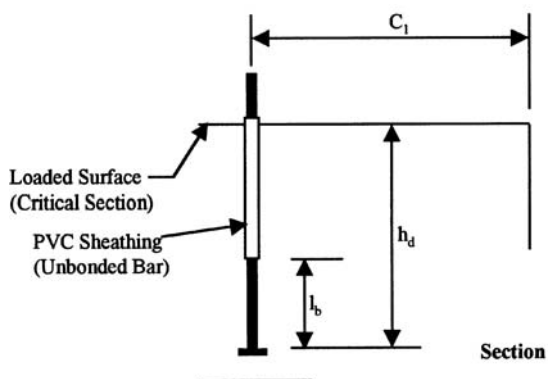


Figure 2-11: Comparison of embedment depth h_d and bonded length l_b in concrete (Adapted from DeVries et al., 1999)

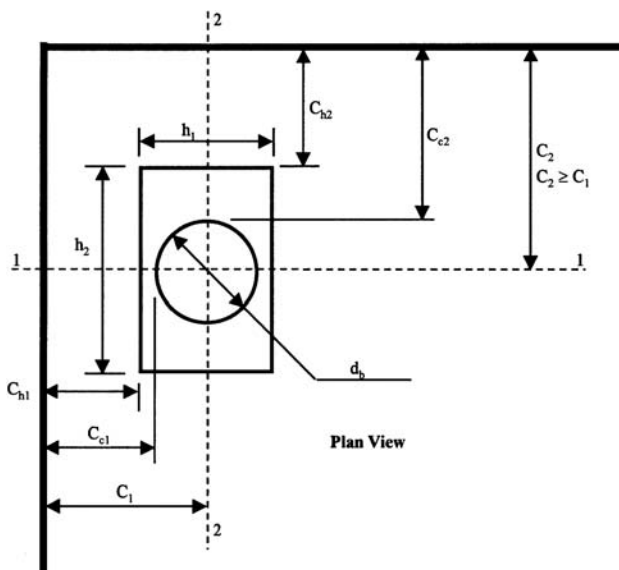


Figure 2-12: Edge distance and head parameters (Adapted from DeVries et al., 1999)

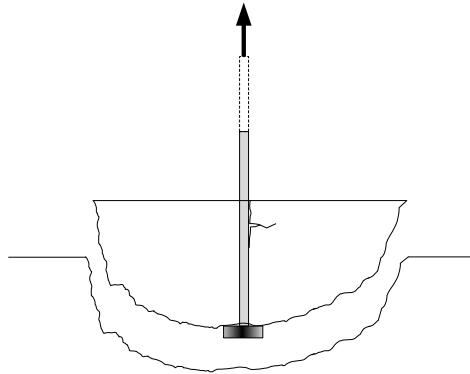


Figure 2-13: Pullout cone failure

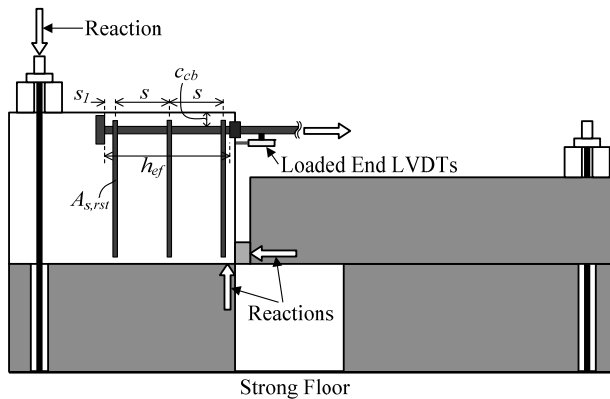


Figure 2-14: Schematic of test specimen and setup (Reproduced; Wright and McCabe, 1997)

Wright and McCabe (1997) conducted 70 beam-end specimens test at the University of Kansas to investigate the performance of headed reinforcement. Three main types of reinforcement were used for test configuration which included straight bars, 180-degree hooked bars, and headed bars to better make comparisons and show the efficiency of using headed bar. These studies recommend the development length for headed bars along with some other specifics such as the location of heads and the amount of head-restraining reinforcement required to prevent prying action of headed bars placed near the concrete-free surface. Figure 2-14 represents the schematic of test apparatus.

ACI 352R-02 (2002) defines two different development lengths of headed bars as functions of $(f_y d_b / \sqrt{f'_c})$ for Type 1 and Type 2 beam-column connections. A Type 2 connection is defined to have sustained strength under deformation reversals into the inelastic range, whereas a Type 1 connection is defined as a connection designed with no consideration of significant inelastic deformation. The critical section for Type 2 connections is defined to be located at the outer edge of joint transverse reinforcement, and at the joint-member interface for Type 1 connections. Furthermore, as the concrete bearing capacity is substantially higher in the diagonal compressive strut, ACI 352R-02 (2002) (Section 4.5.3.2 and Figure 4-9) recommends that a head be located within 50 mm (2 in.) from the back of the joint core (see Figure 2-15). For details of the head, ACI 352R-02 (2002) refers to ASTM A970/A970M-98 (1998), where the net bearing area A_{brg} was recommended to be greater than $9A_b$. The current version of ASTM A970/A970M (2007) no longer specifies a minimum A_{brg} .

To provide the state-of-the-art information on headed reinforcement, ACI Committee 408, Development and Splicing of Deformed Bars, and ACI Committee 439, Steel Reinforcement, are jointly preparing a new report on Headed Ends for Anchorage and Development of Reinforcing Bars. In this report, a broad overview of mechanical anchorage and headed bars is provided, including definitions, historical development, and descriptions of various types of headed end devices, as well as previous research and applications. This report refers to ACI 352R-02 (2002) for the use of headed bars in beam-column connections.

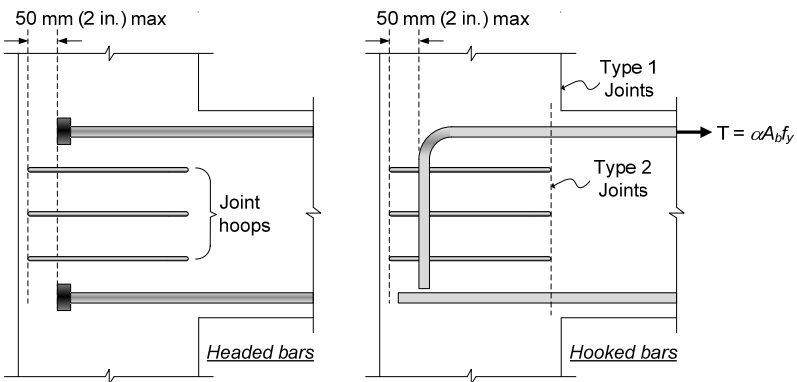


Figure 2-15: Location of headed and hooked bars (Reproduced from ACI 352-02, 2002)

2.2.1 Part II: Experimental Research

The previous tests, 77 of which are Japanese publications written in Japanese, included 69 interstory exterior connections, 17 (T-shaped) roof-interior connections, and 7 knee connections (Kang et al., 2009). There are only a few available reports on these seismic tests published in English (Bashandy, 1996; Wallace et al., 1998; Chun et al., 2007; Lee and Yu, 2009; Kang et al., 2010).

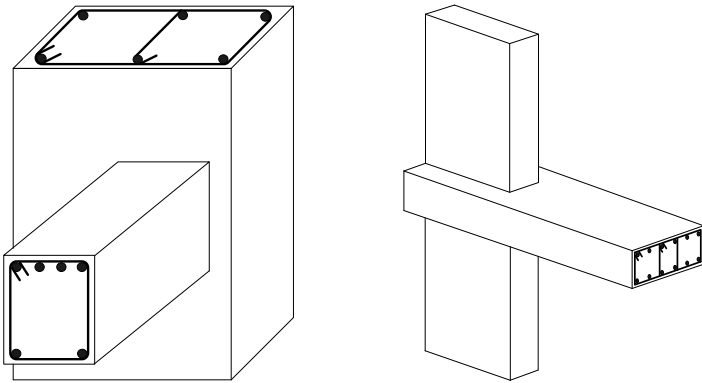
For the exterior connections, headed bars were employed for top and bottom beam reinforcement while they were used for the column reinforcement in the roof-interior connections. Most of the subassemblies were planar without any transverse beam or slab; only a small number of the exterior connections included one or two transverse beam(s) framing perpendicular to the main beam into the column. Two of the exterior connections (Matsushima et al., 2000) had one beam at each of the two principal directions of the rectangular-shaped column, and they were loaded in a combination of the two directions. Of the exterior connection studies, one (Ishida et al., 2007) investigated the performance of headed bars used in a wide beam-column connection in which some of the headed bars were anchored in a transverse beam outside the connection. One (Lee and Yu, 2009) was an eccentric exterior connection. Figure 2-16 represents the schematic diagrams of the investigated beam-column connections. Almost half of the specimens had multiple layers of headed bars in the beam(s) or the column.

The main test variables included the development length for headed bars, clear cover to headed bars, type of anchoring devices, and head size, as well as the compressive strength of concrete and joint failure mode. The development length provided for headed bars ranged widely from $6d_b$ to $23.7d_b$, when measured from the joint-member interface. In most specimens, the net head bearing area A_{brg} was 2.6 to 8 times the reinforcing bar area A_b .

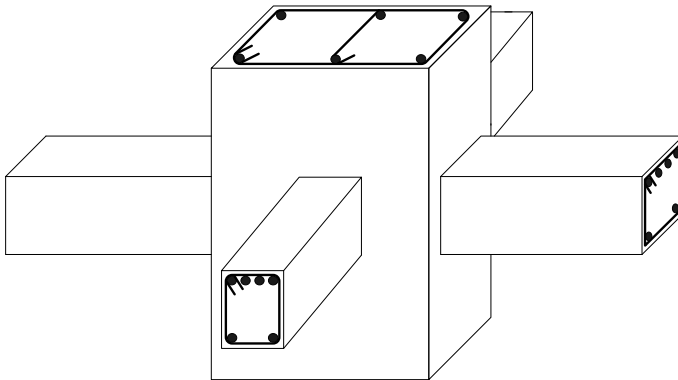
The tested compressive strength of concrete ranged approximately from 24 to 138 MPa (3.5 to 20 ksi), and it was higher than 69 MPa (10 ksi) in approximately 1/4 of the specimens. The tested clear bar spacing c_s in a layer varied from $1.2d_b$ to $7.6d_b$, which was typically not treated as a variable among the specimens in each program.

The performance of headed bars used for beams and/or columns, terminated in the joint cores, was investigated for all types of joint failure modes including beam or column hinging, joint shear failure, and bar bond-slip. Other investigated design variables included the number of beam and/or column bars, the amount of joint transverse reinforcement, the type of reinforcing steel, and the level of column compression. The

tested yield strength of steel ranged from 297 to 1,020 MPa (43 to 148 ksi), and was higher than 690 MPa (100 ksi) in approximately 1/3 of the specimens. Approximately 1/2 of all specimens were tested with large-diameter headed bars (No. 8 to 11; $d_b = 25$ to 36 mm). The pre-applied column compression varied from 0 to 12% of the column gross section area times the measured concrete compressive strength ($f'_{c, meas}$).



(a) Eccentric exterior beam-column connection (b) Wide beam-column connection



(c) Interior beam-column connection

Figure 2-16: Schematic diagrams of investigated beam-column connections